

See discussions, stats, and author profiles for this publication at: <https://www.researchgate.net/publication/230570839>

# White-Light Emitting Microtubes of Mixed Organic Charge-Transfer Complexes

ARTICLE *in* ADVANCED MATERIALS · OCTOBER 2012

Impact Factor: 17.49 · DOI: 10.1002/adma.201201493 · Source: PubMed

---

CITATIONS

34

---

READS

36

7 AUTHORS, INCLUDING:



L. S. Liao

Soochow University, Suzhou, China

181 PUBLICATIONS 3,232 CITATIONS

SEE PROFILE

# White-Light Emitting Microtubes of Mixed Organic Charge-Transfer Complexes

Yi-Long Lei, Yue Jin, Dong-Ying Zhou, Wei Gu, Xiao-Bo Shi, Liang-Sheng Liao,\*  
and Shuit-Tong Lee\*

Supramolecular self-assembly of functional organic molecules, such as wires, rods, and tubes, has attracted ever-increasing attention owing to the molecules' unique electronic and photonic properties.<sup>[1–4]</sup> To date, while there have been extensive studies on single component micro/nanostructures, investigations on multi-component composite micro/nanostructures of different materials are rare. Composite organic micro/nanostructures formed by joining two or more organic materials were shown to be technologically more advantageous in many cases, such as tunable emission,<sup>[5–8]</sup> optical switches,<sup>[9]</sup> and p–n junctions,<sup>[10]</sup> than their respective single component materials. Supramolecular interactions including hydrogen bonding,  $\pi$ – $\pi$  stacking, and charge-transfer (CT) interactions have been used to obtain self-assembly of different components.<sup>[6–9,11]</sup> Nevertheless, only limited success in co-assembly has been achieved due to structural mismatch between diverse molecules, which would induce phase segregation and inhibit their self-assembly. Typically, rational design of each component is required to achieve self-assembly.<sup>[6–12]</sup> For example, a co-assembly system comprising a truxene derivative (Tr3) and its oxidized counterpart (TrO3) has been developed by an electron donor–acceptor interaction in which the structure and shape of the two components are highly similar.<sup>[11]</sup> From this viewpoint, exploring a complementary multi-component system with similar molecular structures is an appropriate approach to achieve composite micro/nanostructures.

On the other hand, it is known that high-performance white-light emission (WLE) is useful to practical applications of organic solid-state lighting sources and full-color displays with reasonable sizes.<sup>[13–18]</sup> In particular, the ordered self-assembly of diverse chromophores for WLE is also drawing much attention due to its potential applications as a micro/nano lighting source, optical detector, optical waveguide, or other micro/nanodevices. For example, white-light emissive waveguides based on doped crystalline nanowires of 9,10-diphenylanthracene (DPA) have been constructed by introducing a phosphorescent dopant, iridium(III) bis(2-phenyl benzothiazolato-N,C<sup>2'</sup>)-

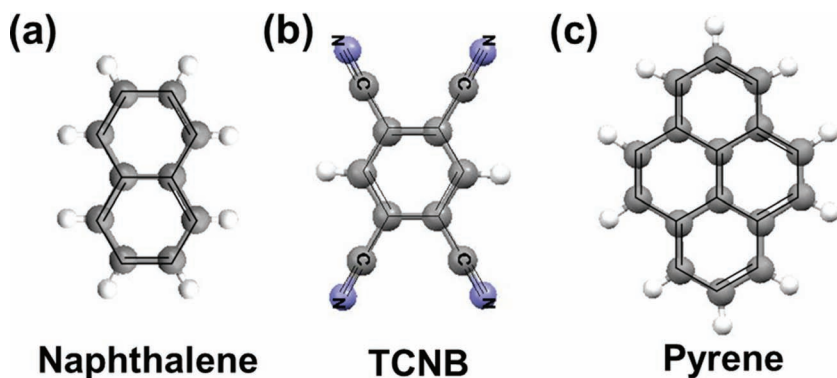
acetylacetonate ((BT)<sub>2</sub>Ir(acac)), into a blue emitting host.<sup>[19]</sup> However, the previous reports on white-light emissive composite micro/nanostructures mainly focused on traditional fluorescent or phosphorescent dyes, and crystalline CT complexes with strong fluorescence are rarely reported or studied. Significantly, the modular structure of CT complexes allows the modification of and control over crystal structure and optical properties by altering CT interactions between electron donors and acceptors. For instance, a typical electron acceptor, 1,2,4,5-tetracyanobenzene (TCNB), can form a series of luminescent CT complexes with aromatic electron donors, such as naphthalene, phenanthrene, and pyrene, which exhibit intense multi-color emission from blue through green to red.<sup>[20–22]</sup> In contrast to aggregation-induced quenching, these luminescent materials are non-emissive in dilute solution, but become highly emissive in the solid state, which may be regarded as a type of aggregation-induced emission enhancement (AIEE).<sup>[23,24]</sup> Therefore, a luminescent CT complex may be a promising candidate considering its high solid-state luminescence efficiency.<sup>[20–22,25–27]</sup> In addition, those two-component molecules in a TCNB-based CT complex system are nearly planar, and stacked alternately on each other, which prompts us to investigate whether co-assembly of CT complexes with similar structures emitting in blue and red colors can be built to generate white light.

In this communication, we first report the controlled synthesis of one-dimensional (1D) single crystalline microtubes of a naphthalene–TCNB complex by CT-induced assembly with the assistance of solvent etching. Remarkably, 1D microtubes of the naphthalene–TCNB complex exhibit highly efficient blue emission owing to an AIEE effect. Furthermore, self-assembled microtubes of mixed CT complexes comprising TCNB and naphthalene are also formed with pyrene as dopant. Indeed, pyrene can be efficiently incorporated into a naphthalene–TCNB complex by replacing naphthalene molecules, which may be favored by a CT interaction between pyrene and TCNB, and  $\pi$ – $\pi$  stacking between naphthalene–TCNB and pyrene–TCNB. Highly efficient Förster resonance energy transfer (FRET) from the excited naphthalene–TCNB to pyrene–TCNB molecules is obtained in mixed CT complex microtubes. The mixed CT complex microtubes can be tailored to exhibit emission in pure white or other desired colors by adjusting the dopant concentration. Furthermore, we first demonstrate that white-light emissive CT complex microtubes can serve as active optical waveguides. This simple solution-phase multi-component self-assembly provides an alternative approach to construct miniaturized luminescent devices from CT complexes.

Dr. Y.-L. Lei, Y. Jin, D.-Y. Zhou, W. Gu, X.-B. Shi,  
Prof. L.-S. Liao, Prof. S.-T. Lee  
Jiangsu Key Laboratory for Carbon-Based  
Functional Materials and Devices  
Institute of Functional Nano and Soft Materials (FUNSOM)  
Soochow University  
Suzhou, Jiangsu 215123, China  
E-mail: lsiao@suda.edu.cn; apannale@suda.edu.cn



DOI: 10.1002/adma.201201493



**Scheme 1.** Molecular structures of a) naphthalene, b) 1,2,4,5-tetracyanobenzene (TCNB), and c) pyrene.

Herein, naphthalene and pyrene were selected as electron donors and TCNB as an electron acceptor (**Scheme 1**) to synthesize luminescent CT complexes. As shown in **Figure 1**, microstructures derived from a CT complex consisting of naphthalene and TCNB were first prepared by solution-processed self-assembly. In brief, a stock solution of naphthalene ( $C_N = 20$  mM) was mixed rapidly with an equal volume of TCNB solution ( $C_T = 20$  mM) in acetonitrile under vigorous stirring. After several minutes, the resultant solution (2.5 mL) was injected into 10 mL of a mixed solvent of ethanol and water ( $V_{\text{ethanol}}: V_{\text{H}_2\text{O}} = 1:3$ ). A light-colored flocculent precipitate appeared within several

seconds and was left undisturbed for 30 min. **Figure 1a** and **b** show typical scanning electron microscopy (SEM) images of the as-prepared 1D microstructures of the naphthalene–TCNB complex at different magnification ratios. It reveals clearly that 1D hollow tubular structures with a rectangular cross section were obtained, as confirmed by the single end-opened tube (solid circle). Meanwhile, a small hole appears near the end of the 1D microstructure, offering additional evidence of tube formation (dashed circle). Each individual tube has a length of hundreds of micrometers and a diameter of  $\sim 3$   $\mu\text{m}$ . The tubular structure of the naphthalene–TCNB complex can be further demonstrated by the transmission electron microscopy (TEM)

image, as shown in **Figure 1c**, which reveals that a single microtube has an inner diameter of  $\sim 1.3$   $\mu\text{m}$  and wall thickness of  $\sim 700$  nm. Additionally, the corresponding selected area electron diffraction (SAED) pattern is shown in the inset of **Figure 1c**. Combined with the powder X-ray diffraction (XRD) patterns simulated based on the bulk crystals of the naphthalene–TCNB complex (**Figure S1**, Supporting Information), the SAED pattern could be indexed with lattice constants obtained from a monoclinic cell:  $a = 9.39$  Å,  $b = 12.66$  Å,  $c = 6.87$  Å,  $\alpha = 90^\circ$ ,  $\beta = 107.2^\circ$ , and  $\gamma = 90^\circ$ . Furthermore, it can be concluded that the 1D microtubes have single crystal structures growing along the [001] direction. **Figure 1d** displays the molecular packing in a naphthalene–TCNB crystal, revealing strong  $\pi$ – $\pi$  stacking and primary growth along the C axis, i.e., the [001] direction. The preferential growth along the [001] direction could be induced by a CT interaction between the donor naphthalene and the acceptor TCNB, which is responsible for the formation of 1D microstructures.

As we know, the degree of saturation is a predominant factor in controlling the morphology and monodispersity of the products, and several methods, such as absorbent-assisted physical vapor deposition (PVD) and colloid chemical reaction,<sup>[5,28]</sup> have been developed to achieve this purpose. For example, manipulation of the growth kinetics has been achieved by adjusting the concentration of  $\text{ZnTPP} \cdot \text{H}_2\text{O}$  growth units, and consequently the kinetics of supersaturation for crystallization, thus yielding organic nanocrystals (ONCs) with well-controlled sizes and shapes.<sup>[28]</sup> Inspired by these successes, we introduce a mixed solvent of ethanol and water as a poor solvent to control the supersaturation in solution-processed self-assembly so as to control the morphology and uniformity of the naphthalene–TCNB complex. Since naphthalene–TCNB molecules are insoluble in water (and slightly soluble in ethanol), if only water was used

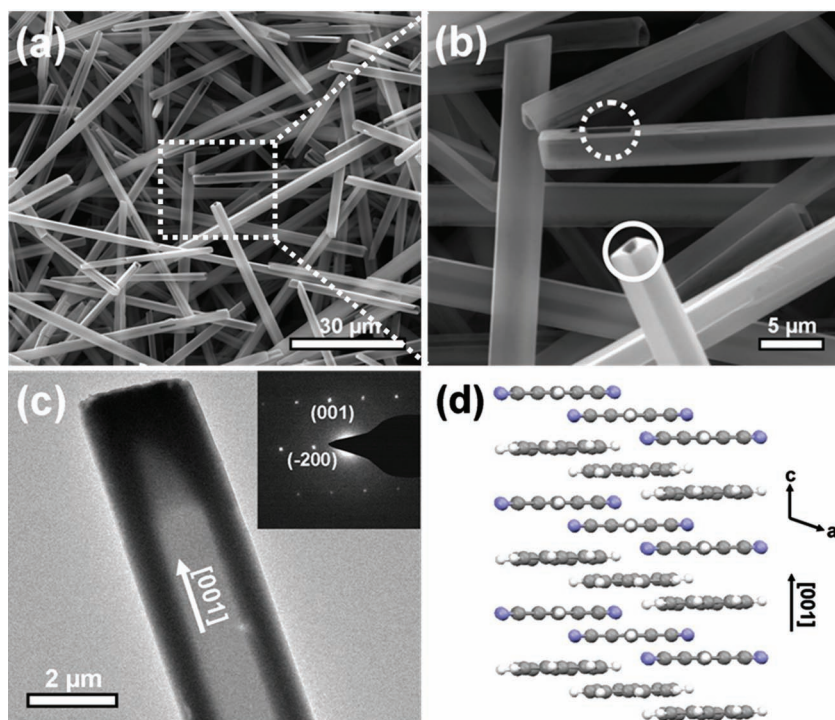


**Figure 1.** SEM images of the CT complex of naphthalene–TCNB microtubes at a) low and b) high magnification. Solid circle shows single end-opened tube, dashed circle shows single hollow tube with small hole. c) TEM image of a typical CT complex microtube. Inset shows the corresponding SAED pattern. d) Molecular packing of the CT complex of naphthalene–TCNB along the C axis, i.e., the [001] direction.

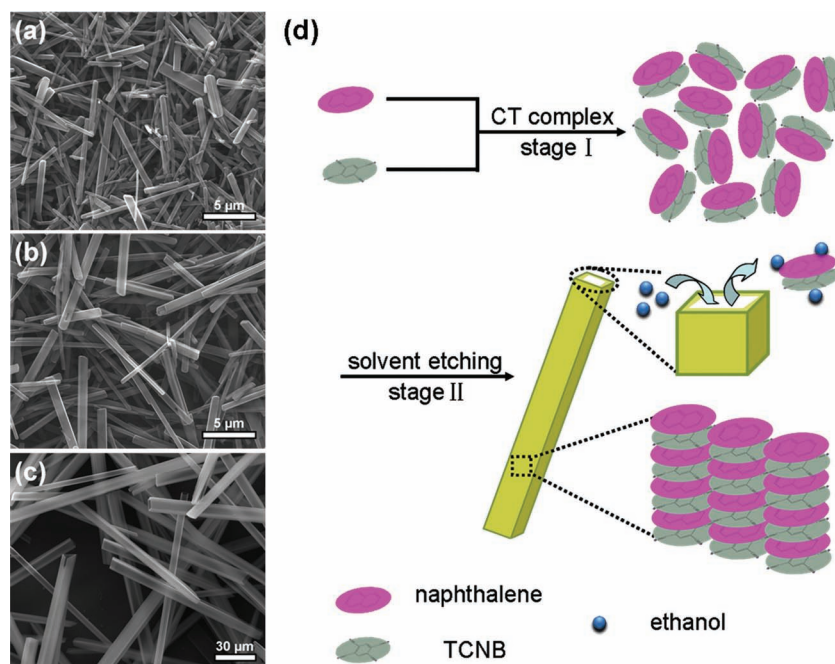


**Figure 2.** SEM images of 1D microtubes of the naphthalene–TCNB complex obtained with the volume ratio of ethanol and water ( $V_{\text{ethanol}}: V_{\text{H}_2\text{O}}$ ) set to 0: 10 (a), 1: 9 (b), and 4: 6 (c). d) Schematic illustration of the possible formation mechanism for 1D naphthalene–TCNB microtubes.

as a poor solvent, a stable colloid dispersion would be formed instantly and irregular solid micro/nanorods would be obtained, as shown in **Figure 2a**. If a mixed solvent containing ethanol and water was used as a poor solvent, supersaturation would be reached slowly due to its higher solubility, and hence the uniformity of the CT complex micro/nanostructures would be easier to control in the mixed solvent. **Figure 2b** shows that the uniformity of 1D micro/nanostructures of the naphthalene–TCNB complex indeed improved significantly when the volume ratio of ethanol and water changed to 1: 9. In addition, a small amount of microtubes also appeared. At a volume ratio of 4: 6, well-defined rectangular microtubes with larger diameters of 7.5 μm were readily obtained (**Figure 2c**). Systematic investigation showed the optimal ratio of  $V_{\text{ethanol}}: V_{\text{H}_2\text{O}} = 1: 3$  for the preparation of CT complex microtubes with uniform sizes (**Figure 1**). Obviously, it can be seen that the morphology transformation from solid micro/nanorods to hollow microtubes can be achieved successfully when the volume ratio of ethanol to water was increased gradually.

According to the above experimental results, a possible formation mechanism for 1D microtubes of the naphthalene–TCNB complex is proposed, as shown in **Figure 2d**. A stable CT complex solution in acetonitrile consisting of naphthalene as the donor and TCNB as the acceptor was first synthesized at room temperature (stage I). Subsequently, the homogeneous CT complex solution was quickly introduced into a poor solvent of ethanol and water. A solvent exchange interaction between acetonitrile and the poor solvent would induce the naphthalene–TCNB molecules to aggregate as a result of its high concentration (10 mM). The two-component molecules are nearly planar, and stacked alternately along the C axis in the bulk crystal of

the naphthalene–TCNB complex, which is consistent with the molecular packing of the CT complex (**Figure 1d**). In the present process, CT interactions between naphthalene and TCNB would drive the preferential growth of the naphthalene–TCNB molecules along the [001] direction (C axis), thus favoring the formation of 1D naphthalene–TCNB microstructures. However, it is worth noting that only solid micro/nanorods of the naphthalene–TCNB complex were obtained if ethanol wasn't introduced into a poor solvent, as shown in **Figure 2a**. Thus, it can be concluded that, instead of acetonitrile, pre-existing ethanol in the poor solvent should be responsible for the formation of tubular structures. In particular, a high density of defects at the rod center, as reported to exist at the center of [2-(*p*-dimethylaminophenyl)ethenyl]phenylmethylenepropanedinitrile (DAPMP) nanorods,<sup>[29]</sup> could lead to the formation of tubular structures by an etching process by the solvent action of THF. Similarly, the solvent etching or dissolution of naphthalene–TCNB molecules by ethanol would occur upon injecting the naphthalene–TCNB complex solution in acetonitrile into a mixed solvent of ethanol and water (stage II).

A high etching rate at the rod center would be achieved and induce the morphology evolution of the CT complex from solid micro/nanorods to tubular microstructures. In addition, crystals are grown more slowly when ethanol was introduced as an etching agent, which would lead to the larger size and higher-quality crystallization of the final microtubes compared to that of the solid micro/nanorods without ethanol.

Different CT complex microtubes can also be synthesized by the present CT-induced assembly strategy with the assistance of solvent etching. The tubular structures would remain unchanged when a prototypical donor, pyrene, was used to form a CT complex with TCNB (**Figure S2**, Supporting Information). Remarkably, it can be seen that a suspension of naphthalene–TCNB complex microtubes is highly blue-emissive but becomes non-emissive in acetonitrile solution, excited with a UV lamp (365 nm) in **Figure 3a**. This type of behavior is consistent with the features of an AIEE effect, which suggests that a solid environment is needed to reduce rapid internal conversion and recombination in solution, as reported previously.<sup>[22]</sup> The solid-state photoluminescence (PL) efficiency for the blue-emissive microtubes suspension of the naphthalene–TCNB complex is measured at 17.5%. Similar to the naphthalene–TCNB complex, a suspension of pyrene–TCNB complex microtubes also exhibits a typical AIEE effect. However, only weak orange emission is observed because the pyrene–TCNB molecules cannot be excited effectively by UV light, which is supported by the excitation and emission spectra of a suspension of pyrene–TCNB complex shown in **Figure 3b**. Meanwhile, **Figure 3b** also displays the excitation and emission spectra of a suspension of naphthalene–TCNB complex microtubes. The fluorescence spectrum of the naphthalene–TCNB complex exhibits a good



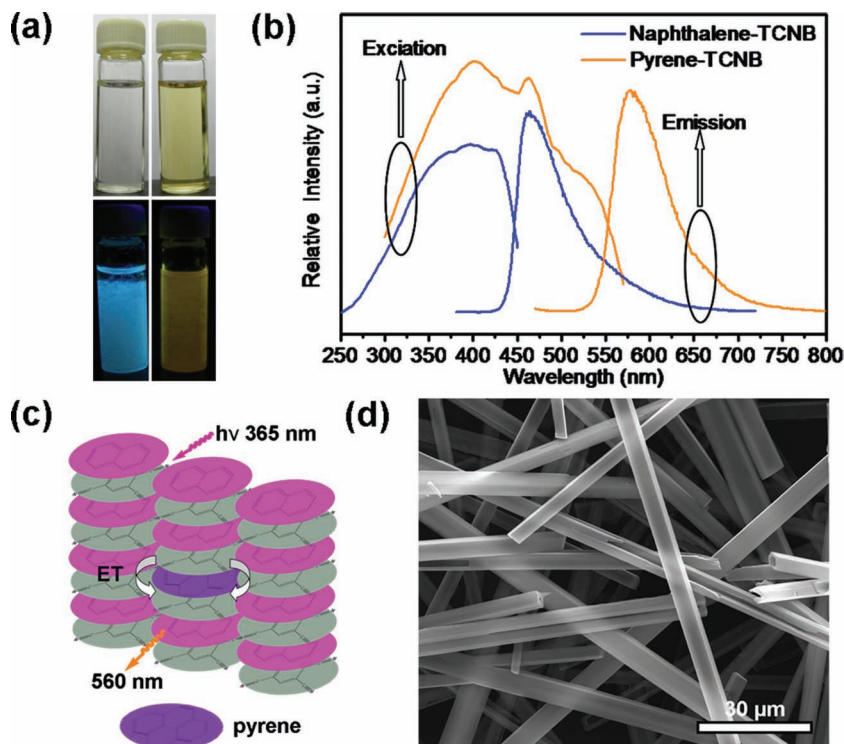


**Figure 3.** a) Photographs of naphthalene-TCNB and pyrene-TCNB molecules in acetonitrile solution in daylight (upper row) and their corresponding microtube suspensions under a UV lamp (365 nm, bottom row). b) Excitation and emission spectra of 1D microtubes of naphthalene-TCNB (blue) and pyrene-TCNB (orange) complexes. The excitation wavelength is 365 nm. c) Schematic representation of the energy transfer in doped CT complex microtubes. d) SEM image of mixed CT complex microtubes with a doping concentration of 0.015%.

overlap with the excitation spectrum of the pyrene-TCNB complex in the wavelength range of 400–550 nm, which may result in the occurrence of Förster-type energy transfer between them. In addition, we expect that pyrene could be introduced into the naphthalene-TCNB complex by replacing naphthalene molecules based on a CT interaction between pyrene and TCNB and  $\pi$ - $\pi$  stacking between naphthalene-TCNB and pyrene-TCNB, when small amounts of pyrene are used as dopant. Thus we attempt to extend this concept to two-component CT complex microtubes consisting of naphthalene and pyrene as donors and TCNB as acceptor so as to obtain WLE by an effective energy transfer process. The schematic representation in Figure 3c shows a possible energy transfer process, in which the excited naphthalene-TCNB transfers energy to pyrene-TCNB. As a consequence, the blue emission is partially quenched, whereas the orange emission is enhanced accordingly. In fact, tunable emission could be achieved in mixed CT complex microtubes by adjusting the dopant concentration. In addition, Figure 3d clearly demonstrates that the rectangular tubular structures of the mixed CT complex do not change when a doping concentration of 0.015% is adopted.

To investigate whether pyrene can be incorporated into a naphthalene-TCNB complex matrix, fluorescence microscopy tests of mixed CT complex microtubes with different doping concentration were performed. Figure 4 shows the fluorescence microscopy images of the doped microtubes dried on a quartz slide, excited with unfocused UV light (330–380 nm). Figure 4a shows that pure or undoped naphthalene-TCNB complex microtubes exhibit bright blue PL, which is attributed to a typical CT transition between the electron donor of naphthalene and the electron acceptor of TCNB.<sup>[20–22]</sup> Remarkably, at a doping concentration of merely 0.015% of pyrene, the blue-emissive CT complex microtubes change to uniform white-light emission, as shown in Figure 4b. Laser confocal fluorescence microscopy (LCFM) images (Figure S4, Supporting Information) show clearly that pyrene molecules were dispersed uniformly in the naphthalene-TCNB complex matrix. Figure S4 reveals that when these white-emitting microtubes were excited with a 405 nm laser, intense blue and orange PL can be observed, respectively. The orange emission originating from direct excitation of the pyrene-TCNB component at 405 nm is hardly detected due to the low concentration of pyrene (about  $1.5 \times 10^{-3}$  mM) in the microtubes. Thus, it is inferred that energy transfer from the excited naphthalene-TCNB to pyrene-TCNB, rather than the AIEE effect

of pyrene-TCNB molecules, was responsible for the significant fluorescence enhancement of the orange emissive region in the white emissive microtubes. At a pyrene concentration of 0.1% (Figure 4c), heterogeneous microtubes containing an orange-emissive body and blue-emissive ends were obtained, which are in contradiction to the uniform morphologies observed by SEM (Figure S3, Supporting Information). LCFM images of the same sample further confirm that the main body displays

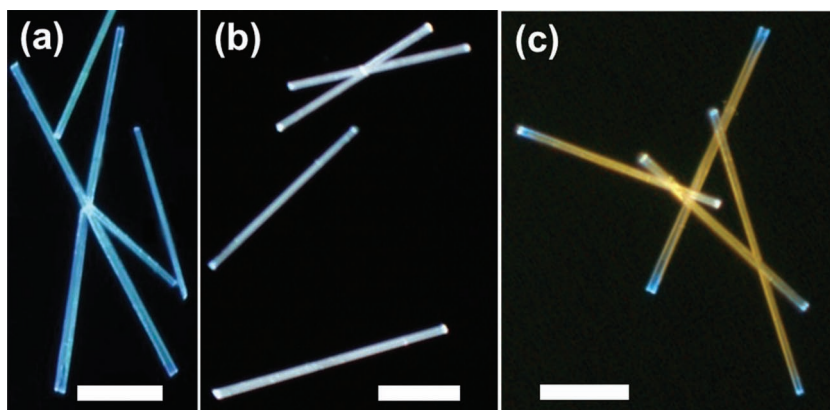


**Figure 4.** Fluorescence microscopy images of mixed CT complex microtubes with a doping concentration of a) 0, b) 0.015%, and c) 0.1% excited with unfocused UV light (330–380 nm). All scale bars are 30 μm.

uniform orange PL, whereas the ends emit strong blue PL (Figure S5, Supporting Information). Interestingly, the doped CT complex microtubes exhibit bright PL spots at the ends of each microtube, thus suggesting that the ordered crystalline CT complex microtubes may serve as a promising active optical waveguide medium.<sup>[32]</sup>

Even after small amounts of pyrene as dopant are introduced, the powder XRD patterns of the mixed CT complex microtubes deposited on the surface of a quartz substrate demonstrate that they are still highly crystalline in nature and mainly related to the naphthalene–TCNB component (Figure S1, Supporting Information). In fact, no XRD characteristics of the pyrene–TCNB component were identified even when the doping concentration is up to 0.1%. On the basis of the XRD pattern results, it can be further proved that pyrene molecules were well-dispersed in the naphthalene–TCNB complex microtubes at a doping concentration of 0.015%. When the doping concentration increased to 0.1%, we found that pyrene molecules were dispersed uniformly in the bodies of the naphthalene–TCNB complex microtubes, instead of the two ends. This difference may be due to the fact that the association constant between pyrene and TCNB is distinctly different from that between naphthalene and TCNB,<sup>[31]</sup> thus resulting in the selective deposition of pyrene with increasing doping concentration. Furthermore, it is well known that besides extensive spectral overlap, a desirable distance of ~2–6 nm between energy donor and acceptor is essential to achieve an efficient energy transfer process.<sup>[9,32]</sup> In the current doping system, well-dispersed pyrene molecules in the naphthalene–TCNB complex matrix enable a suitable distance between donor and acceptor, which facilitates efficient energy transfer from the excited naphthalene–TCNB to pyrene–TCNB molecules.

The mixed CT complex microtube films obtained from different doping ratios, and spin-coated on a quartz substrate also exhibit intense fluorescence when excited with a UV lamp, as shown in the inset of Figure 5a. Blue, white, and orange colors can be obtained readily by adjusting the doping concentration. Similar to pure naphthalene–TCNB complex microtubes, highly efficient fluorescence should be attributed to an AIEE effect in the doping system. The steady-state spectroscopic studies were also carried out to examine the optical properties of the doped CT complex microtube films. In Figure 5a, the spectrum (blue curve) from an undoped naphthalene–TCNB microtube film shows a broad structureless band at ~460 nm excited with 365 nm, which originates from a CT transition from the HOMO of naphthalene to the LUMO of TCNB.<sup>[26]</sup> At 0.015% pyrene concentration, the spectrum (white curve) from white-light emissive film displays an additional band at 556 nm, corresponding to the typical emission of pyrene–TCNB molecules. The CIE coordinate calculated from the spectrum (white curve)

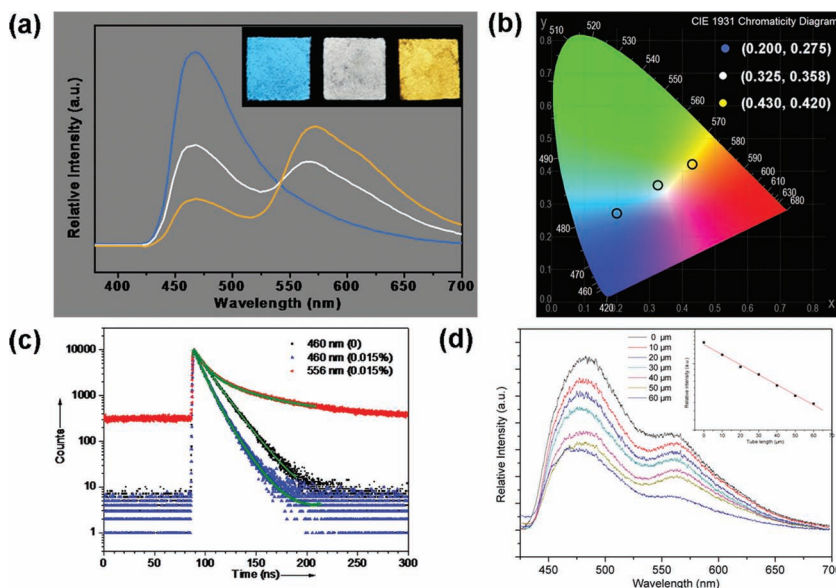


**Figure 5.** a) Steady state emission spectra of mixed CT complex microtube films spin-coated on a quartz substrate at a doping concentration of 0 (blue), 0.015% (white), and 0.1% (orange) upon excitation with 365 nm. The excitation wavelength is 365 nm. b) Emission colors in a CIE 1931 chromaticity diagram: 0 (blue), 0.015% (white), and 0.1% (orange). c) Time-resolved fluorescence decay of mixed CT complex microtubes at different doping concentration excited with a 370 nm laser. d) Spatially resolved PL spectra of out-coupled light for a single white-light emitting microtube recorded by excitation at a distance of 0–60  $\mu\text{m}$  from the left end. Inset shows the logarithmic plots of relative intensities of PL peaks at 560 nm versus distance between excitation and out-coupling for the PL spectra.

is (0.325, 0.358), which is close to ideal white-light (0.33, 0.33) (Figure 5b). As the doping ratio increased to 0.1%, the spectrum (orange curve) shows that emission of naphthalene–TCNB molecules is suppressed, whereas that of pyrene–TCNB molecules is enhanced greatly, demonstrating that efficient energy transfer could occur from the naphthalene–TCNB donor to the pyrene–TCNB acceptor. Besides the naphthalene–TCNB band at 460 nm, the emission spectrum of the film excited at 365 nm exhibits that the PL of pyrene–TCNB is slightly red-shifted to around 563 nm. Time-resolved fluorescence decay profiles of both the undoped and the doped CT complex microtubes deposited on a quartz substrate, are presented in Figure 5c. The monoexponential lifetime measured for the pure naphthalene–TCNB complex microtubes is calculated to be 14.9 ns and it is shortened to 13.8 (66.7%) and 7.6 ns (33.3%) by doping of pyrene (0.015%). These results further confirm energy transfer from naphthalene–TCNB to pyrene–TCNB in the doped CT complex microtubes. Remarkably, the solid-state PL efficiency for the white-light emissive microtube film is measured at 15.7%. The luminescence efficiency of the microtube film is fairly stable even after exposure to air for about two months at room temperature. The mixed CT complex microtubes may be a potential candidate for waveguide materials considering their high solid-state luminescence efficiency, as shown in Figure 4. To confirm this, propagation loss was also studied using scanning near-field optical microscopy (SNOM) by collecting the spatially resolved PL spectra of the waveguiding emission out-coupled at one end of a single white-light emitting microtube

upon excitation with a 408 nm laser. Figure S7 (Supporting Information) shows a series of PL images of a microtube when moving the excitation spot along the microtube length from left to right. Remarkably, the PL spots can only be observed from both ends of the tubes besides at the local area of the excited position, which is a typical characteristic of strong waveguiding behavior. Figure 5d shows the dependence of the intensity of waveguiding PL out-coupled at the left end of the microtube as a function of the propagation distance. The naphthalene–TCNB PL at the blue-emissive region upon local excitation, and the pyrene–TCNB PL at 560 nm as a result of FRET, decrease with increasing the propagation length. The PL intensity of the end emission at 560 nm decays almost linearly following the increase of propagation length, as shown in the inset of Figure 5d, suggesting the CT microtubes can act as a typical active waveguide. Besides direct contact between the substrate and a facet of the microtube, Rayleigh scattering caused by possible compositional inhomogeneities and structural defects should be responsible for the optical propagation losses of the microtubes along their 1D directions.<sup>[3,32,33]</sup>

In summary, 1D single-crystalline microtubes of naphthalene–TCNB CT complexes with rectangular cross section have been synthesized by etching-assisted CT-induced self-assembly. The CT complex microtubes exhibit highly efficient blue emission due to a remarkable AIEE effect. We further extend the self-assembly approach to preparing mixed naphthalene–TCNB complex microtubes containing pyrene as dopant. By tuning the pyrene concentration, the mixed CT complex microtubes can be tailored to exhibit emission from blue through pure white to orange due to efficient energy transfer between the energy donor and acceptor. The present self-assembly synthesis of mixed CT complexes presents a facile and low-cost approach to construct white light-emitting composite organic micro/nano-structures. The strategy could provide a new insight to understand and research luminescent CT complex systems, which may have potential application in optoelectronics.

## Experimental Section

**Materials Synthesis:** Solvents and all other chemicals were obtained from commercial sources and were used without further treatment. One-dimensional microtubes of naphthalene–TCNB complexes with blue emission were prepared by solvent etching-assisted self-assembly. In a typical synthesis, 10 mL of a stock solution of naphthalene ( $C_N = 20$  mM) was mixed rapidly with an equal volume of TCNB solution ( $C_T = 20$  mM) in acetonitrile under vigorous stirring. After several minutes, the resultant solution (2.5 mL) was injected into 10 mL of a mixed solvent of ethanol and water ( $V_{\text{ethanol}}: V_{\text{H}_2\text{O}} = 1: 3$ ). A light-colored flocculent precipitate appeared within several seconds. Furthermore, mixed CT complex microtubes were also synthesized following a similar experimental procedure, using a different concentration of pyrene. In the current experimental process, the molar ratio ( $N$ ) between pyrene and naphthalene molecules can be calculated, according to  $N = C_P/C_N$ . For example, the white-light emissive CT complex microtubes can be synthesized with a doping concentration of 0.015% ( $C_P = 1.5 \times 10^{-3}$  mM). The resultant colloidal samples were collected on the surface of a quartz substrate. Meanwhile, part of the flocculent colloid was separated by centrifugation at 6000 rpm and washed several times with ultrapure water, and finally dried under vacuum for further analysis.

**Materials Characterization:** The morphologies and sizes of the mixed CT complex samples were examined using field-emission scanning

electron microscopy (FESEM, FEI Quanta 200F) at acceleration voltages of 10–15 kV. Prior to analysis, the samples were coated with a thin gold layer using an Edwards Sputter Coater. TEM images were obtained using a Philips CM 200 electron microscope operated at an accelerating voltage of 80 kV. One drop of the as-prepared colloidal dispersion was deposited on a carbon-coated copper grid, and dried under high vacuum. The X-ray diffraction (XRD) patterns were measured by a D/max 2400 X-ray diffractometer with Cu K $\alpha$  radiation ( $\lambda = 1.54050$  Å) operated in the  $2\theta$  range from  $3^\circ$  to  $30^\circ$ , by using the samples of CT complex microtubes filtered on the surface of a quartz substrate. The steady-state fluorescence and excitation spectra of doped CT complex microtubes were measured on a HORIBA JOBIN YVON FLUOROMAX-4 spectrofluorimeter with a slit width of 1 nm. Meanwhile, the time-resolved fluorescence decay of these samples was also measured. The samples were both deposited on the surface of a quartz substrate. The fluorescence microscopy images were obtained using a Leica DMRBE fluorescence microscope with a spot-enhanced charge couple device (CCD, Diagnostic Instrument, Inc.). The samples were prepared by placing a drop of dispersion onto a cleaned quartz slide. Laser confocal fluorescence microscopy (Leica, TCS-SP5) equipped with a near ultraviolet laser (405 nm) was used for fluorescent images of mixed CT complex microtubes. The microarea PL images of a single white-light emitting microtube were record by scanning near-field optical microscopy (NSOM, Alpha, Witec). The microtube was excited with a focused laser (408 nm).

## Supporting Information

Supporting Information is available from the Wiley Online Library or from the author.

## Acknowledgements

This work was supported by the Natural Science Foundation of China (No. 61036009, No. 21161160446, No. 61177016 and No. 51072126), the National “863” Project of China (No. 2011AA03A110) and the Natural Science Foundation of Jiangsu Province (No. BK2010003). This work was also funded by the Priority Academic Program Development of Jiangsu Higher Education Institutions (PAPD).

Received: April 13, 2012

Revised: June 13, 2012

Published online: July 26, 2012

- [1] K. Takazawa, Y. Kitahama, Y. Kimura, G. Kido, *Nano Lett.* **2005**, 5, 1293.
- [2] Y. S. Zhao, A. D. Peng, H. B. Fu, Y. Ma, J. N. Yao, *Adv. Mater.* **2008**, 20, 1661.
- [3] Y. S. Zhao, J. J. Xu, A. D. Peng, H. B. Fu, Y. Ma, L. Jiang, J. N. Yao, *Angew. Chem. Int. Ed.* **2008**, 47, 7301.
- [4] A. L. Briseno, S. C. B. Mannsfeld, M. Roberts, X. M. Lu, Y. J. Xiong, S. A. Jenekhe, Z. N. Bao, Y. N. Xia, *Nano Lett.* **2006**, 7, 668.
- [5] Y. S. Zhao, H. B. Fu, F. Q. Hu, A. D. Peng, W. S. Yang, J. N. Yao, *Adv. Mater.* **2008**, 20, 79.
- [6] C. Giansante, G. Raffy, C. Schäfer, H. Rahma, M. T. Kao, A. G. L. Olive, A. D. Guerso, *J. Am. Chem. Soc.* **2011**, 133, 316.
- [7] K. P. Tseng, F. C. Fang, J. J. Shyue, K. T. Wong, G. Raffy, A. D. Guerso, D. M. Bassani, *Angew. Chem. Int. Ed.* **2011**, 50, 7032.
- [8] R. Abbel, R. Weegen, W. Pisula, M. Surin, P. Leclère, R. Lazzaroni, E. W. Meijer, A. P. H. J. Schenning, *Chem. Eur. J.* **2009**, 15, 9737.
- [9] Q. Liao, H. B. Fu, C. Wang, J. N. Yao, *Angew. Chem. Int. Ed.* **2011**, 123, 5044.



- [10] Y. J. Zhang, H. L. Dong, Q. X. Tang, S. Ferdous, F. Liu, S. C. B. Mannsfeld, W. P. Hu, A. L. Briseno, *J. Am. Chem. Soc.* **2010**, 132, 11580.
- [11] J. Y. Wang, J. Yan, L. Ding, Y. G. Ma, J. Pei, *Adv. Funct. Mater.* **2009**, 19, 1746.
- [12] A. G. L. Olive, A. D. Guerzo, C. Schäfer, C. Belin, G. Raffy, C. Giansante, *J. Phys. Chem. C* **2010**, 114, 10410.
- [13] Y. Chen, J. Au, P. Kazlas, A. Ritenour, H. Gates, M. McCreary, *Nature* **2003**, 423, 136.
- [14] Y. Sun, N. C. Giebink, H. Kanno, B. Ma, M. E. Thompson, S. R. Forrest, *Nature* **2006**, 440, 908.
- [15] Q. Wang, J. Q. Ding, D. G. Ma, Y. X. Cheng, L. X. Wang, X. B. Jing, F. S. Wang, *Adv. Funct. Mater.* **2009**, 19, 84.
- [16] G. Schwartz, S. Reineke, K. Walzer, K. Leo, *Appl. Phys. Lett.* **2008**, 92, 053311.
- [17] S. Park, J. E. Kwon, S. H. Kim, J. Seo, K. Chung, S. Y. Park, D. J. Jang, B. M. Medina, J. Gierschner, *J. Am. Chem. Soc.* **2009**, 131, 14043.
- [18] S. H. Kim, S. Park, J. E. Kwon, S. Y. Park, *Adv. Funct. Mater.* **2011**, 21, 644.
- [19] C. Zhang, J. Y. Zheng, Y. S. Zhao, J. Yao, *Adv. Mater.* **2011**, 23, 1380.
- [20] N. Mataga, Y. Murata, *J. Am. Chem. Soc.* **1969**, 91, 3144.
- [21] M. V. Koz'menko, M. G. Kuz'min, *J. Appl. Spectrosc.* **1977**, 27, 1129.
- [22] R. J. Dillon, C. J. Bardeen, *J. Phys. Chem. A* **2011**, 115, 1627.
- [23] Y. Hong, J. W. Y. Lam, B. Z. Tang, *Chem. Commun.* **2009**, 4332.
- [24] Y. Hong, J. W. Y. Lam, B. Z. Tang, *Chem. Soc. Rev.* **2011**, 40, 5361.
- [25] S. Masuo, Y. Yamane, T. Endo, S. Machida, A. Itaya, *J. Phys. Chem. C* **2009**, 113, 11590.
- [26] N. Hosaka, M. Obata, M. Suzuki, T. Saiki, K. Takeda, M. Kuwata-Gonokami, *Appl. Phys. Lett.* **2008**, 92, 113305.
- [27] N. Mataga, Y. Murata, *J. Am. Chem. Soc.* **1969**, 91, 3144.
- [28] L. T. Kang, H. B. Fu, X. Q. Cao, Q. Shi, J. N. Yao, *J. Am. Chem. Soc.* **2011**, 133, 1895.
- [29] X. J. Zhang, X. H. Zhang, X. M. Meng, W. S. Shi, C. S. Lee, S. T. Lee, *Angew. Chem. Int. Ed.* **2007**, 46, 1525.
- [30] M. D. Gujrati, N. S. S. Kumar, A. S. Brown, B. Captain, J. N. Wilson, *Langmuir* **2011**, 27, 6554.
- [31] M. Hardouin-Lerouge, P. Hudhomme, M. Sallé, *Chem. Soc. Rev.* **2011**, 40, 30.
- [32] Q. Liao, H. B. Fu, J. N. Yao, *Adv. Mater.* **2009**, 21, 4153.
- [33] X. H. Yan, Y. Su, J. B. Li, J. Früh, H. Möhwald, *Angew. Chem. Int. Ed.* **2011**, 50, 11186.